Local, submicron, strain gradients as the cause of Sn whisker growth

M. Sobiech,[1,2,a)] M. Wohlschlögel,[1] U. Welzel,[1] E. J. Mittemeijer,[1,a)] W. Hügel,[2] A. Seekamp,[2] W. Liu,[3,a)] and G. E. Ice[4]
[1]*Max Planck Institute for Metals Research, Heisenbergstrasse 3, D-70569 Stuttgart, Germany*
[2]*Robert Bosch GmbH, Dieselstrasse 6, D-72770 Reutlingen, Germany*
[3]*Advanced Photon Source, Argonne National Laboratory, Argonne, Illinois 60439, USA*
[4]*Oak Ridge National Laboratory, Oak Ridge, Tennessee 37831-6118, USA*

(Received 21 April 2009; accepted 11 May 2009; published online 2 June 2009)

It has been shown experimentally that local *in-plane residual strain gradients* occur around the root of spontaneously growing Sn whiskers on the surface of Sn coatings deposited on Cu. The strain distribution has been determined with synchrotron white beam micro Laue diffraction measurements. The observed *in-plane residual strain gradients* in combination with recently revealed *out-of-plane residual strain-depth gradients* [M. Sobiech *et al.*, Appl. Phys. Lett. **93**, 011906 (2008)] provide the driving forces for whisker growth. © *2009 American Institute of Physics*. [DOI: 10.1063/1.3147864]

The mechanisms of spontaneous formation and growth of Sn whiskers from surfaces of Sn coatings deposited on Cu represent a controversially discussed phenomenon for more than 50 years.[1,2] As nowadays the system Sn–Cu will usually be applied for interconnection of electronic systems, filamentary Sn whiskering on Sn coated leadframe legs of modern microelectronic devices constitutes an issue of great technological relevance because whisker-induced short-circuit failures have resulted in enormous costs including failures of satellites and military and medical devices.[1]

Sn whiskers are "nearly" perfect single crystal filamentary structures[3,4] (see Fig. 1) with diameters of $\sim 1-10$ μm and with lengths up to several millimeters. Whiskers grow through continuous addition of material to their base[5] with growth rates of around 0.1 nm/s[6] and up to 1000 nm/s in the presence of externally applied mechanical stresses.[4] Despite of 50 years of study, no proposed model to date is capable of explaining all key features of whisker growth behavior on Sn thin films deposited on Cu[2,6–13] (e.g., moment of whiskering, location of nucleation sites, kinetics of growth, and development of specific surface morphologies). The driving force for whisker growth has been attributed by the majority of researchers to a buildup of mechanical compressive strains in the Sn coating during and/or after layer production and thus whisker growth can be regarded as a strain relief phenomenon.[2,7–9,13–16] Compressive strains in the Sn coating develop upon aging at room temperature due to intermetallic phase formation at the Cu/Sn interface. After Sn deposition and during subsequent aging at room temperature, Cu diffuses into the Sn thin film[14,17] leading to the formation of the intermetallic compound Cu_6Sn_5,[14] preferentially along the Sn grain boundaries intersecting the Cu/Sn interface.[2,8,18] The Cu_6Sn_5 formation is accompanied by a volume expansion and as a consequence, residual compressive strains parallel to the surface can be generated in the Sn thin film.[2,8,18] It has been speculated that negative strain gradients either in the direction from the Sn surface toward the intermetallic compound region near the interface with the substrate[1,2,8,14,18] (i.e., the strain becomes less compressive toward the Sn surface) or parallel to the surface of the Sn layer in the direction from the whisker root toward the whisker surroundings (i.e., the strain becomes less compressive toward the whisker root), drive the transport of Sn atoms to the whisker root and thus control Sn whisker growth.[2,19] However, conclusive experimental evidence for the presence or absence of strain gradients has remained elusive.

Only very recently, experimental evidence has been presented which indicates that compressive strains are not a prerequisite for whisker formation, but that, instead, the strain *gradient* in the direction from the surface of the Sn layer to the intermetallic compound region must be negative.[20] Thus, whisker growth can occur in the presence of a tensile strain in the surface region of the Sn layer.

A previous attempt to assess the residual strain distribution around a Sn whisker using the white beam Laue diffraction technique[19] suffered from low experimental accuracy for strain detection. Moreover, the present work demonstrates that it is of paramount importance to conduct strain characterization around the whisker *during its ongoing growth*, otherwise the locally acting driving force(s) are likely absent. In this letter, we discuss the role of *in-plane residual strain gradients* determined experimentally around the root of

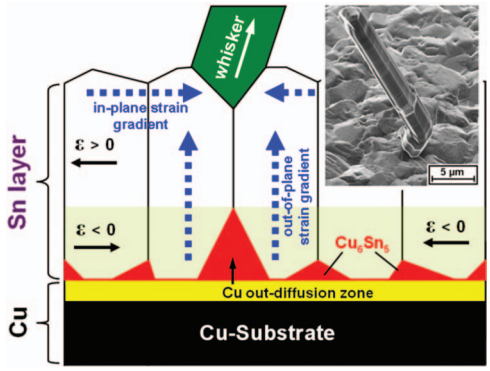

FIG. 1. (Color) Schematic model, on the basis of the results of the present work, of the whisker-formation process in Sn thin films deposited on Cu substrates upon aging at room temperature. The focused ion beam micrograph illustrates the growth morphology of a Sn whisker.

[a)]Authors to whom correspondence should be addressed. Electronic addresses: m.sobiech@mf.mpg.de, e.j.mittemeijer@mf.mpg.de, and wjliu@anl.gov.

growing Sn whiskers in combination with recently revealed *out-of-plane residual strain-depth gradients*[20] (see section above) as driving forces for whisker growth.

In the present work, Sn thin films with a thickness of about 3 μm were electrodeposited onto pure Cu substrates (commercial leadframe material) using an industrial electrolyte by employing a laboratory electrodeposition setup. The Sn layer has a {321}-fiber texture and a columnar Sn grain morphology with in-plane grain sizes of 2–5 μm (for further details see Ref. 18). Directly after Sn deposition the surface of the specimens was rinsed with methanol and subsequently the specimens were dried and aged at room temperature (i.e., storage at ~22 °C/25%–50% relative humidity without controlling the ambient atmosphere). The first whiskers were observed roughly 4 days after Sn deposition.

In order to experimentally determine the strain distribution around growing Sn whiskers, high-resolution white beam micro Laue diffraction measurements were performed at the synchrotron beamline 34ID-E[21] at the Advanced Photon Source (APS) of the Argonne National Laboratory (Argonne, Illinois, USA). The region around the root of growing Sn whiskers covering an area of $\sim 20 \times 20$ μm^2 was step scanned (with steps of 0.5 μm steps using a *x-y* translation stage) with a polychromatic (8–24 keV) focused x-ray beam of $\sim 0.3 \times 0.3$ μm^2. Since the size of the Sn grains is larger than the focused x-ray beam, a single crystal micro-diffraction Laue pattern was recorded for each probed specimen position. In combination with a high-precision charge coupled device (CCD) area detector for data collection, two dimensional (i.e., the diffraction data recorded at each probed specimen position contain information from all positions along the penetration depth through the film thickness of around 3 μm) residual strain measurements were performed on the basis of white beam Laue diffraction. By using computer-automated peak search routines the angular positions of the Bragg reflections were determined and by employing pattern-recognition software the diffraction pattern could be indexed with respect to reference patterns.[22] The crystallographic orientation and the (deviatoric) strain tensor components were derived directly from the indexed Laue diffraction patterns. The accuracy of this method depends strongly on the experimental setup and on the resolution of the CCD detector used for the measurement. In the present study, the diagonal (deviatoric) strain tensor components could be determined with an accuracy of about 0.01% strain.

After aging the specimen at room temperature for around 40 days, two dimensional micro-diffraction measurements were made around the root of growing Sn whiskers. The crystallographic orientation map and the corresponding diagonal (deviatoric) strain tensor components measured at each probed position in the vicinity of a whisker root (see Fig. 3) are shown in Fig. 2. Also shown are the radially averaged values of these strain tensor components around the whisker root. Off-diagonal components are not shown due to significantly higher strain uncertainty.

The in-plane strain tensor components ε_{xx} and ε_{yy} can be used to calculate the (averaged) in-plane (parallel to the specimen surface) strain $\varepsilon_{\parallel}$ ($\varepsilon_{\parallel}=1/2\ (\varepsilon_{xx}+\varepsilon_{yy})$; see Figs. 2(e) and 2(f)). The diagonal (deviatoric) strain tensor component ε_{zz} (strain component normal to the specimen surface) can also be used to assess the (averaged) in-plane strain due to

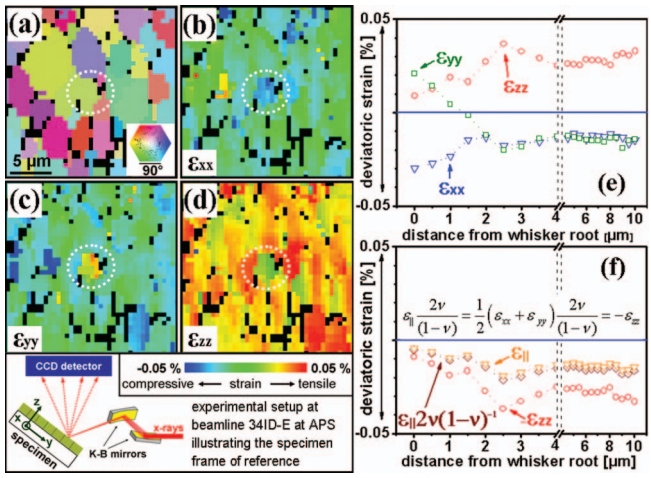

FIG. 2. (Color) Two dimensional micro-diffraction (area of ~20 $\times$20 μm^2) data taken around the root (white dotted circle) of a growing Sn whisker. The regions colored black correspond to not indexed data points. (a) The orientation image displays the corresponding (RGB) color-coded crystallographic orientations of the [001] axis of the Sn grains with respect to the [001] pole (which has the white color-code). [(b)–(d)] Color-coded diagonal (deviatoric) strain tensor components ε_{xx}, ε_{yy} and ε_{zz} (see the illustration of the beamline setup and indication of the specimen frame of reference at the bottom of the figure). The scale bar displays the color-coded deviatoric strains. (e) Radially, in the plane of the surface, averaged values of all diagonal (deviatoric) strain tensor components (ε_{xx}, ε_{yy}, and ε_{zz}) as function of the distance from the whisker root. (f) Radially averaged in-plane strain $\varepsilon_{\parallel}$ as function of the distance from the whisker root in comparison with the radially averaged values of $\varepsilon_{\parallel}2\nu(1-\nu)^{-1}$ and $-\varepsilon_{zz}$.

mechanical equilibrium conditions by taking the (isotropic) Poisson's ratio of Sn (ν=0.36; in this work the isotropic Poisson's ratio of Sn has been calculated from single crystal elastic constants[23] by adopting the elastic grain interaction model of Eshelby–Kröner[24]) into account. The radial averaging of the strains over differently orientated (mechanically anisotropic, tetragonal) Sn grains justifies the use of the isotropic Poisson's ratio. As here an in-plane state of stress has to be considered the following relations hold for the corresponding strain: $\varepsilon_{\parallel}2\nu(1-\nu)^{-1}=1/2\ \ (\varepsilon_{xx}+\varepsilon_{yy})\ \ 2\nu(1-\nu)^{-1}=-\varepsilon_{zz}$. The comparison of the thus calculated values for $\varepsilon_{\parallel}2\nu(1-\nu)^{-1}$ with the measured values for the (averaged) in-plane strain $-\varepsilon_{zz}$ clearly confirms data consistency (see Fig. 2(f)).

The residual (out-of-plane) strain ε_{zz} is less tensile at the whisker nucleation site than in the surroundings of the whisker root (see Figs. 2(d) and 2(e)), i.e., the in-plane strain, $\varepsilon_{\parallel}$ (see Fig. 2(f)), is less compressive at the whisker root than in the whisker surroundings. (Note that because deviatoric strain components have been determined, the nature (absolute value) of the strain is unknown.) It must be emphasized that this finding was confirmed by performing measurements for several (i.e., five) growing Sn whiskers (time-resolved scanning electron microscopy (SEM) investigations allowed to prove their ongoing growth behavior), whereas whisker-free specimens upon the same room temperature aging conditions did *not* exhibit either in-plane nor out-of-plane residual strain gradients (whisker-free specimens were produced by applying a post-plating annealing treatment of 150 °C for 1 h,[18] called "post-bake" in industrial manufacturing). Hence, *negative in-plane (radially averaged) residual strain gradients* occur in the direction from the whisker root toward the whisker surroundings (see Fig. 2(f)), i.e.,

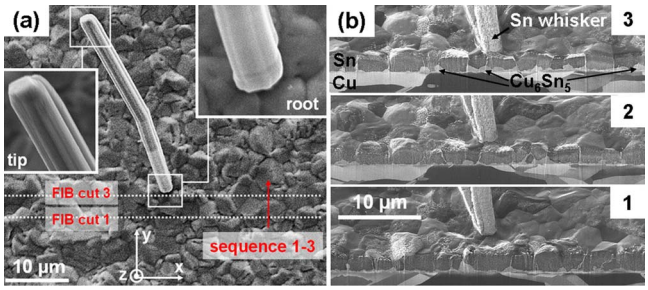

FIG. 3. (Color online) (a) SEM micrographs of the Sn whisker and its surroundings, pertaining to the results shown in Fig. 2. The white dotted lines illustrate the approximate locations of (b) the sequence of cross-sectional FIB micrographs with respect to the specimen frame of reference (cf. Fig. 2).

the strains are more tensile/less compressive at the whisker root.

After aging for about 50 days at room temperature the whisker pertaining to the results shown in Fig. 2 showed a length of about 40 μm and a diameter of about 3 μm (see Fig. 3(a)). Close inspections of the whisker tip during its growth showed that the surface morphology did not change with time, which is compatible with whisker growth by pushing up from the base.[5] In order to reveal the microstructure at the whisker root and near the Cu/Sn interface underneath the Sn whisker, focused ion beam (FIB) cross sections in steps of around 1.2 μm parallel to the surface, progressing toward the whisker root, were prepared sequentially after the last SEM investigation (see Fig. 3(b)). Evidently, the Cu_6Sn_5 formation at the Cu/Sn interface occurs preferentially along the grain boundaries of the columnar grains constituting the Sn layer. The development of Cu_6Sn_5 along Sn grain boundaries is particularly pronounced underneath the whisker root (see Fig. 3(b), image 3). This finding was confirmed by cross-sectional FIB investigations performed on many more Sn whiskers and whisker surroundings.

The measured residual strain distribution and the observed microstructure around the whisker root lead to the following proposal for the mechanism of whisker formation (see also Fig. 1): The deep penetration of Cu_6Sn_5 along the Sn grain boundaries at the Cu/Sn interface induces in-plane compressive (macro) strains in the Sn layer, particularly in the depth range where Cu_6Sn_5 formation along the Sn grain boundaries proceeds. Due to mechanical equilibrium conditions in-plane tensile (macro) strains then occur in the Sn layer close to the surface; most pronouncedly at those surface locations where penetration of Cu_6Sn_5 along Sn grain boundaries is most distinctive, as underneath a whisker. As a consequence, both negative out-of-plane residual strain gradients, in the direction from the surface of the Sn layer to the Cu/Sn interface (for specific experimental evidence, see Ref. 20) and negative *in-plane residual strain gradients* in the direction from the whisker-nucleation site toward the whisker surroundings (see Fig. 2) occur. These out-of-plane and in-plane negative strain gradients provide a driving force for the transport of Sn atoms to the whisker nucleation site, as strain-relief mechanism, and thus lead to Sn whisker growth.

Whiskers do not form at every location at the surface corresponding with a pronounced Cu_6Sn_5 formation underneath, as follows from the cross-sectional FIB micrographs shown in Fig. 3. This may be related to the crystallographically anisotropic nature of (self-)diffusion in Sn. The precise crystallographic orientation of the Sn grains around and above the location with pronounced Cu_6Sn_5 formation co-determines the rate of Sn transport from the strained surroundings to the potential whisker-nucleation site.

In this work, it was shown experimentally by employing high-resolution synchrotron white beam micro Laue diffraction that *negative in-plane residual strain gradients* occur around the root of a growing Sn whisker. These *negative* in-plane residual strain gradients in combination with *negative* out-of-plane residual strain-depth gradients[20] are the cause of transport of Sn atoms to the whisker root, as a strain-relief mechanism. Compressive strain is not a prerequisite for whisker formation. Instead, the nature of the three dimensional strain *gradients* around a potential whisker-nucleation site is decisive for whisker formation.

The authors are much obliged to the company "Hans Heimerdinger Oberflächentechnik" in Pforzheim, Germany for specimen preparation. Use of the Advanced Photon Source was supported by the Office of Basic Energy Sciences, U.S. Department of Energy, under Grant No. DE-AC02-06CH11357. G.E.I. was supported by the Division of Material Sciences and Engineering, Office of Basic Energy Sciences, and U.S. Department of Energy.

[1]G. T. Galyon, IEEE Trans. Electron. Packag. Manuf. **28**, 94 (2005).
[2]K. N. Tu, C. Chen, and A. T. Wu, J. Mater. Sci. Mater. Electron. **18**, 269 (2007).
[3]C. Herring and J. K. Galt, Phys. Rev. **85**, 1060 (1952).
[4]R. M. Fisher, L. S. Darken, and K. G. Carroll, Acta Metall. **2**, 368 (1954).
[5]S. E. Koonce and S. M. Arnold, J. Appl. Phys. **25**, 134 (1954).
[6]W. C. Ellis, D. F. Gibbons, and R. C. Treuting, in *Growth and Perfection of Crystals*, edited by R. H. Doremus, B. W. Roberts, and D. Turnbull (Wiley, New York, 1958), pp. 102–120.
[7]U. Lindborg, Acta Metall. **24**, 181 (1976).
[8]B. Z. Lee and D. N. Lee, Acta Mater. **46**, 3701 (1998).
[9]R. R. Hasiguti, Acta Metall. **3**, 200 (1955).
[10]J. Franks, Acta Metall. **6**, 103 (1958).
[11]F. C. Frank, Philos. Mag. **44**, 854 (1953).
[12]J. D. Eshelby, Phys. Rev. **91**, 755 (1953).
[13]W. J. Boettinger, C. E. Johnson, L. A. Bendersky, K.-W. Moon, M. E. Williams, and G. R. Stafford, Acta Mater. **53**, 5033 (2005).
[14]K. N. Tu, Acta Metall. **21**, 347 (1973).
[15]E. Chason, N. Jadhav, W. L. Chan, L. Reinbold, and K. S. Kumar, Appl. Phys. Lett. **92**, 171901 (2008).
[16]K. S. Kumar, L. Reinbold, A. F. Bower, and E. Chason, J. Mater. Res. **23**, 2916 (2008).
[17]B. F. Dyson, T. R. Anthony, and D. Turnbull, J. Appl. Phys. **38**, 3408 (1967).
[18]M. Sobiech, U. Welzel, R. Schuster, E. J. Mittemeijer, W. Hügel, A. Seekamp, and V. Müller, Proceedings of the 57th Electronic Components and Technology Conference, Reno, NV, May 29–June 1, 2007 (unpublished), p. 192.
[19]W. J. Choi, T. Y. Lee, K. N. Tu, N. Tamura, R. S. Celestre, A. A. MacDowell, Y. Y. Bong, and L. Nguyen, Acta Mater. **51**, 6253 (2003).
[20]M. Sobiech, U. Welzel, E. J. Mittemeijer, W. Hügel, and A. Seekamp, Appl. Phys. Lett. **93**, 011906 (2008).
[21]G. E. Ice, B. C. Larson, J. Z. Tischler, W. Liu, and W. Yang Mater. Sci. Eng., A **399**, 43 (2005).
[22]J.-S. Chung and G. E. Ice, J. Appl. Phys. **86**, 5249 (1999).
[23]W. F. Gale, *Smithells Metals Reference Book* (Butterworths, London, 2004).
[24]U. Welzel, J. Ligot, P. Lamparter, A. C. Vermeulen, and E. J. Mittemeijer, J. Appl. Crystallogr. **38**, 1 (2005).